ELSEVIER

Materials Science and Engineering A192/193 (1995) 908–913

MATERIALS SCIENCE & ENGINEERING A

# Time–temperature transformation behavior of Ti–24Al–11Nb

L.M. Hsiung, H.N.G. Wadley

*Department of Materials Science and Engineering, University of Virginia, Charlottesville, VA, 22903-2442, USA*

**Abstract**

The time–temperature transformation behavior of a rapidly solidified (RS) Ti–24Al–11Nb alloy has been studied between 450 and 850 °C using X-ray diffraction, electron diffraction, transmission electron microscopy and microindentation methods. A revised isothermal transformation path from the initial B2 to the final $\alpha_2$ structure has been proposed: B2 ($Pm\bar{3}m$)→B19 (Pmma)→O′ (Cmcm)→O′ (Cmcm)→$\alpha_2$ ($P6_3/mmc$). Age-hardening was found to accompany the B2→O′ transitions. The hardness increased to a maximum value of about 5.4 GPa when the microstructure consisted of mostly O′ laths. Further aging resulted in a softening correlated with O′ coalescence and transformation to the $\alpha_2$ phase. The hardness decreased to a minimum value of about 2.6 GPa when the microstructure had evolved to an equiaxed $\alpha_2$ structure. The results reveal that the O′→$\alpha_2$ reaction becomes extremely slow, i.e. the O′ phase is kinetically stabilized, at temperatures below about 500 °C.

*Keywords*: Time–temperature transformation; Titanium; Aluminium; Niobium

## 1. Introduction

Earlier studies of isothermal phase transformations in RS Ti–24at%.Al–11at.%Nb alloys below 850 °C led to the proposal that the supercooled B2 phase, upon isothermal aging, undergoes a sequential phase transition: B2→T (DO3-like phase)→O′ (ordered orthorhombic, previously designated as O)→$\alpha_2$+O ($Ti_2AlNb$) [1]. The B2→O′ transition was also proposed to be a composition-invariant transition, but did require both a partial chemical ordering and a displacive reaction. Because only a very small amount of the (chemically different) equilibrium O ($Ti_2AlNb$) phase can be formed in Ti–24Al–11Nb composition alloys [1], the decomposition reaction, O′→$\alpha_2$+O is simplified hereafter to O′→$\alpha_2$ in this alloy.

Recently, the existence of the DO3-like T phase has been re-examined. Banerjee [2] showed a similarity between electron diffraction patterns of the so-called T phase, and diffraction patterns computed for the equilibrium O (Cmcm, $Ti_2AlNb$) phase based on the crystal structure proposed by Mozer et al. [3], and suggested that the structure of the T phase was not DO3 but orthorhombic. In parallel with this, evidence has recently been obtained that a periodic $\{110\}\langle\bar{1}10\rangle$-type shear (i.e. a shuffling of atoms on alternating $\{110\}$ planes along $\langle\bar{1}10\rangle$ direction) in association with a chemical ordering operates during quenching and aging of the supercooled B2 phase [4]. The atomic shuffling alone alters the stacking sequence of the B2 ($Pm\bar{3}m$) phase to a 2H-type, and transforms the B2 to a B19 (Pmma) phase. Two ordered orthorhombic phases, O″ (Cmcm, previously designated as T) and O′ (Cmcm, previously designated as O), are then sequentially transformed from the B19 phase by the chemical ordering. While detailed work will be published elsewhere [4], two possible paths for the B2→O″ transition are suggested here: (a) an atomic shuffling followed by a partial chemical ordering which enables a B2-(atomic shuffling)→B19-(ordering of Al atoms)→O″ transition to occur, or (b) B2→O″ when both the atomic shuffling and partial chemical ordering take place simultaneously. The O′ phase is then formed by an O″-(ordering of Ti atoms+lattice distortion)→O′ transition. Note that these are similar to a transformation path: B2 ($Pm\bar{3}m$)→B19 (Pmma)→O (Cmcm, ($Ti_2AlNb$)) proposed by Bendersky et al. [5].

Hardness measurements on samples aged in temperature regimes where these transformations occur have revealed the existence of age-hardening/softening phenomena in RS Ti–24Al–11Nb alloys. Age-hardening accompanies the B2→O′ transition, and reached a


*SSDI* 0921-5093(94)03320-X

maximum as the aged samples contained mostly the O′ phase. Subsequent aging resulted in a softening during the O′ → $\alpha_2$ transition. The results are reported here.

## 2. Experimental procedure

A rapidly solidified $(Ti,Nb)_3Al$ alloy with a nominal composition of Ti–24at.%Al–11at.%Nb (Ti–14wt.%Al–21wt.%Nb) was used in this study. Two types of samples were used: powder and foil. The powder was produced from ingot via the plasma rotary electrode process (PREP) by Nuclear Metals Inc., Concord, MA. The chemical composition of the PREP powder was previously reported in Ref. [6]. The foil was produced from powder of identical composition via the inductive-coupled plasma deposition (ICPD) process at GE Aircraft Engines, Lynn, MA. Both the powder and foil samples were examined in their as-prepared and aged status using X-ray diffraction (XRD), transmission electron microscopy (TEM) and electron diffraction techniques. Prior to aging treatments, both the powder and foil samples were wrapped with tantalum foils and encapsulated in cleaned and evacuated quartz ampoules under vacuum (about $10^{-7}$ Torr). Isothermal heat treatments of the PREP powders were performed at temperatures ranging between 450 and 850 °C for different times (1 min to 168 h). Foil samples were aged at 650 °C for different times (10 min to 24 h). All the samples were water-quenched after heat treatment.

TEM specimens were prepared from both the as-deposited and aged foil. Microstructures were examined using a Philips 400T transmission electron microscope. Phase evolution in the powder samples was examined by X-ray diffraction using Cu K$\alpha$ radiation ($\lambda = 1.5406$ Å) in a Scintag XDS-2000 diffractometer operated at 40 kV and 35 mA. The scanning angles ($2\theta$) employed for diffraction ranged from 25° to 75°, with a scanning rate of 2 deg $min^{-1}$. Microhardness measurements were performed at room temperature from powder samples using a MICROMET Vickers-hardness indentor (applied load, 100 gf; dwell time, 35 s). Seven to eleven tests were conducted for each data point. Hardness values with both means and standard deviations are reported.

## 3. Results and discussion

### 3.1. Phase evolution

Although X-ray diffraction (XRD) is a convenient method for studying phase evolution in isothermally aged RS Ti–24Al–11Nb, it suffers from a poor resolution when used to distinguish phases with similar lattice parameters. To compensate for this, electron diffraction has been used in order to identify metastable phases as well as transformation pathway. While detailed work on the identification of various phases will be published elsewhere [4], here we display in Fig. 1 a typical result of the electron diffraction experiment: microdiffraction patterns of the $\langle 110\rangle_{B2}$, $\langle 001\rangle_{B19}$, $\langle 001\rangle_{O''}$, $\langle 001\rangle_{O'}$, and $\langle 0001\rangle_{\alpha 2}$ zones generated from a foil sample after aging at 650 °C for different times. The phase evolution path at 650 °C is revealed to be: B2 → B19 → O″ → O′ → $\alpha_2$. Lattice parameters of the various phases are measured to be: B2, $a = 0.325$ nm; B19, $a = 0.325$ nm, $b = c = 0.46$ nm; O″, $a = 0.66$ nm, $b = 0.92$ nm, $c = 0.46$ nm); O′, $a = 0.605$ nm, $b = 0.98$ nm, $c = 0.473$ nm; $\alpha_2$, $a = 0.58$ nm, $c = 0.465$ nm. These provide a basis for analyzing XRD results.

An XRD pattern generated from an as-prepared powder sample is shown in Fig. 2. Clearly, B2 is the only phase to exist in the as-prepared powder. Note that the superlattice reflections (for example the 111 and 210 reflections) of the B2 phase were too weak to be detected using a Cu K$\alpha$ X-ray source. XRD patterns generated from powder samples after aging at 500, 600 and 700 °C for different times are shown in Figs. 3–5. Throughout the XRD experiment, we found that the B19 and O″ phases were hard to resolve, as a result of overlapping peaks and relatively weak reflection intensity. However, it is interesting to note that a

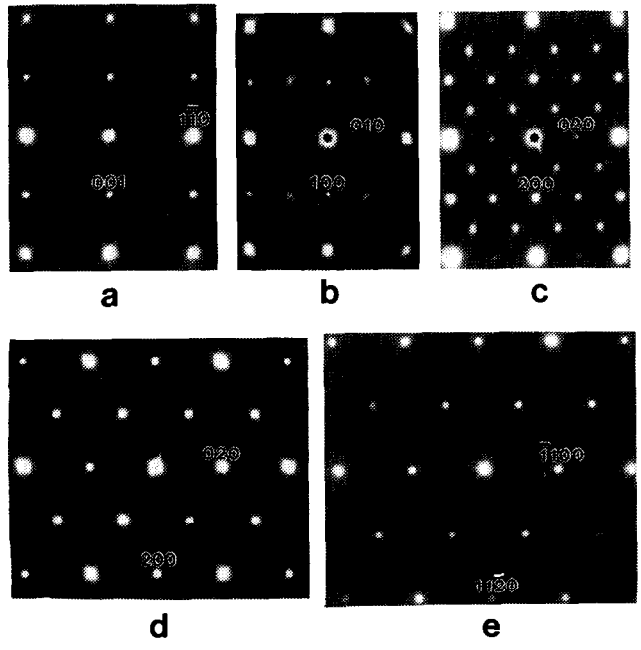


Fig. 1. Microdiffraction patterns generated from foil samples: (a) $\langle 110\rangle_{B2}$ (as-deposited); (b) $\langle 001\rangle_{B19}$ (as-deposited); (c) $\langle 001\rangle_{O''}$ (650 °C, 10 min); (d) $\langle 001\rangle_{O'}$ (650 °C, 2 h); (e) $\langle 0001\rangle_{\alpha 2}$ (650 °C, 24 h).

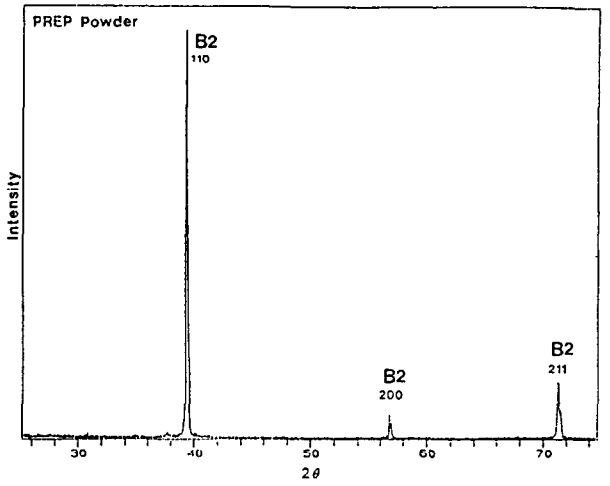


Fig. 2. XRD patterns (Cu Kα showing that B2 phase is the only phase to exist in the as-prepared powder.

tetragonal distortion (about 2%) of the B2 phase was detected (both by electron diffraction and XRD) when the O″ domains were formed within the B2 phase. This is distortion that has been previously reported [1,7] and was at that time rationalized by the formation of the so-called T (tetragonal) phase. A typical example is shown in Fig. 3(a), where the B2 phase was tetragonally distorted (peak splitting) owing to the existence of the O″ phase after aging at 500 °C for 10 min.

The O″→O′ transition occurred when the powder samples were further aged; for example, almost only O′ phase was observed after aging at 500 °C for 1 h (Fig. 3(b)). The O′ phase at 500 °C was more stable and was retained (without transforming to the equilibrium $\alpha_2$ phase) even after a prolonged aging (60 h) at 500 °C (Fig. 3(c)). A similar result was previously reported for a sample after a prolonged aging for 168 h at 450 °C [1]. When samples were aged at temperatures above 500 °C, the O′ phase became unstable, and the O′→$\alpha_2$ transition began. The O′ phase was found to coexist with the $\alpha_2$ phase after aging at 600 °C for 10 min (Fig. 4(a)), whereas samples contained mostly $\alpha_2$ phase after aging for 48 h at 600 °C (Fig. 4(b)) and for 5 h at 700 °C (Fig. 5(b)). Similar results for samples aged at 650 and 850 °C were also previously reported in Ref. [1]. The XRD results clearly indicate that there exists a critical temperature (about 500 °C), below which the O′→$\alpha_2$ reaction becomes very sluggish and the O′ phase becomes kinetically stable.

### 3.2. Age-hardening/softening

Hardness variations in the $(Ti,Nb)_3Al$ system have been reported by several researchers [8–10]. Vickers hardness tests were employed here to study the

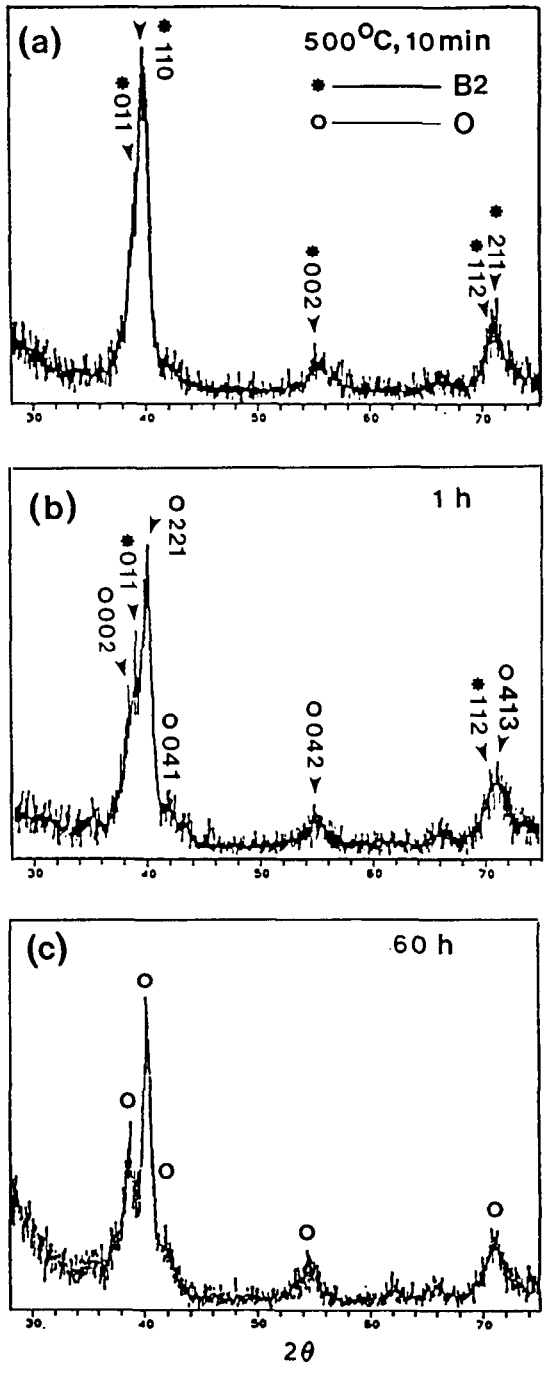


Fig. 3. XRD patterns (Cu Kα generated from powder samples after aging at 500 °C for different times: (a) 10 min; (b) 1 h; (c) 60 h.

mechanical properties associated with the phase evolution. The measured hardness values ranged between 206 HV and 572 HV, where the unit of HV is kgf $mm^{-2}$ (1 kgf $mm^{-2}$ = 9.8 MPa). The size of the indentations was about 20 μm, much larger than the size of phase domains (which were in the nanometer range), and so the data sampled by the microindenta-

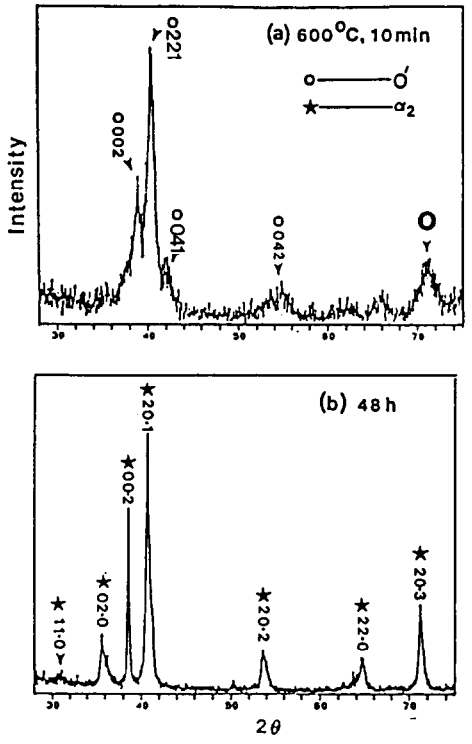


Fig. 4. XRD patterns (Cu Kα generated from powder samples after aging at 600 °C for different times: (a) 10 min; (b) 48 h.

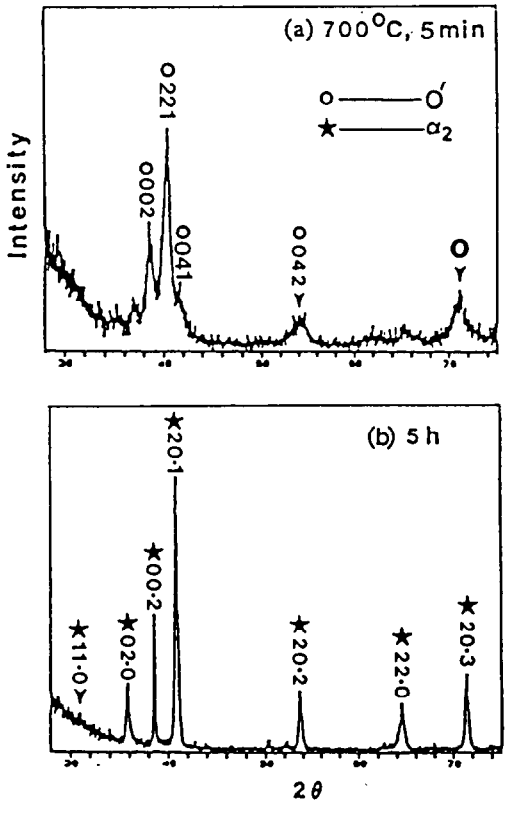


Fig. 5. XRD patterns (Cu Kα generated from powder samples after aging at 700 °C for different times: (a) 5 min; (b) 5 h.

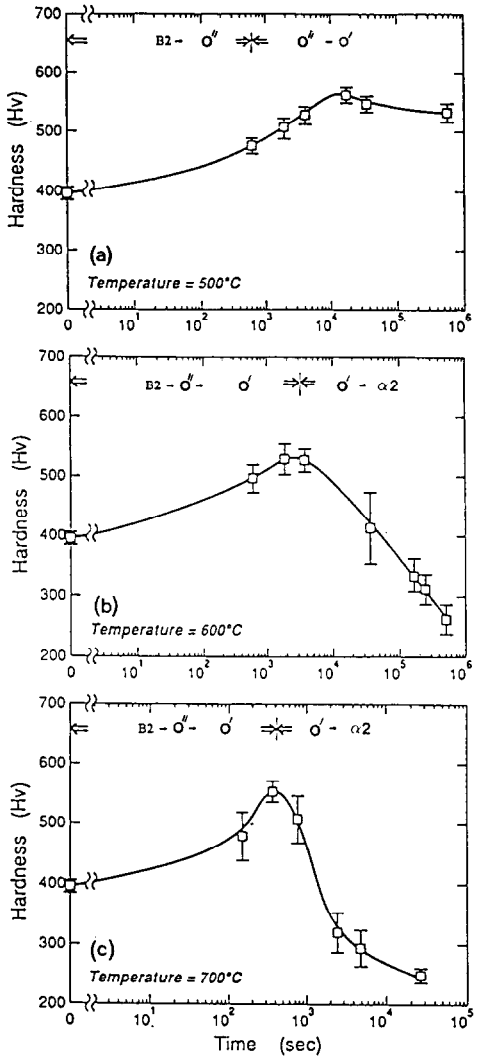


Fig. 6. Hardness variations of powder samples after aging for various times at: (a) 500 °C; (b) 600 °C; (c) 00 °C. The standard deviation is indicatedc by the vertical bars.

tion from a multi-phase region were considered to be a statistically adequate sample of the microstructure. The hardness of the as-prepared powder (containing mostly B2 phase) was about 395 HV (or 3.9 GPa), which corresponds to an estimated yield strength of about 1.3 GPa. The hardness data measured from samples aged at 500, 600 and 700 °C are shown in Fig. 6. For all temperatures studied, the hardness initially increased with increasing aging time, reached a peak value of about 550 HV and then decreased. However, as can be seen in Fig. 6(a), the hardness variation obtained from samples aged at 500 °C showed only a slight decrease (from about 550 HV to about 520 HV) even after prolonged aging. In contrast, for samples aged at 600 and 700 °C (Figs. 6(b) and 6(c)), a significant decrease of hardness occurred after prolonged aging. A comparison between hardness data and XRD results indicates

that an age-hardening took place during the B2→O′ stage of transition, and an age-softening occurred during the O′→$\alpha_2$ transition stage. The result shown in Fig. 6(a) clearly indicates that the O′ phase is stable when aged at temperatures below 500 °C.

While careful work is needed to elucidate the mechanisms of the age-hardening and -softening behavior, here we correlate the age-hardening/softening behavior to the microstructural evolution as visualized in Fig. 7. The hardness variation obtained

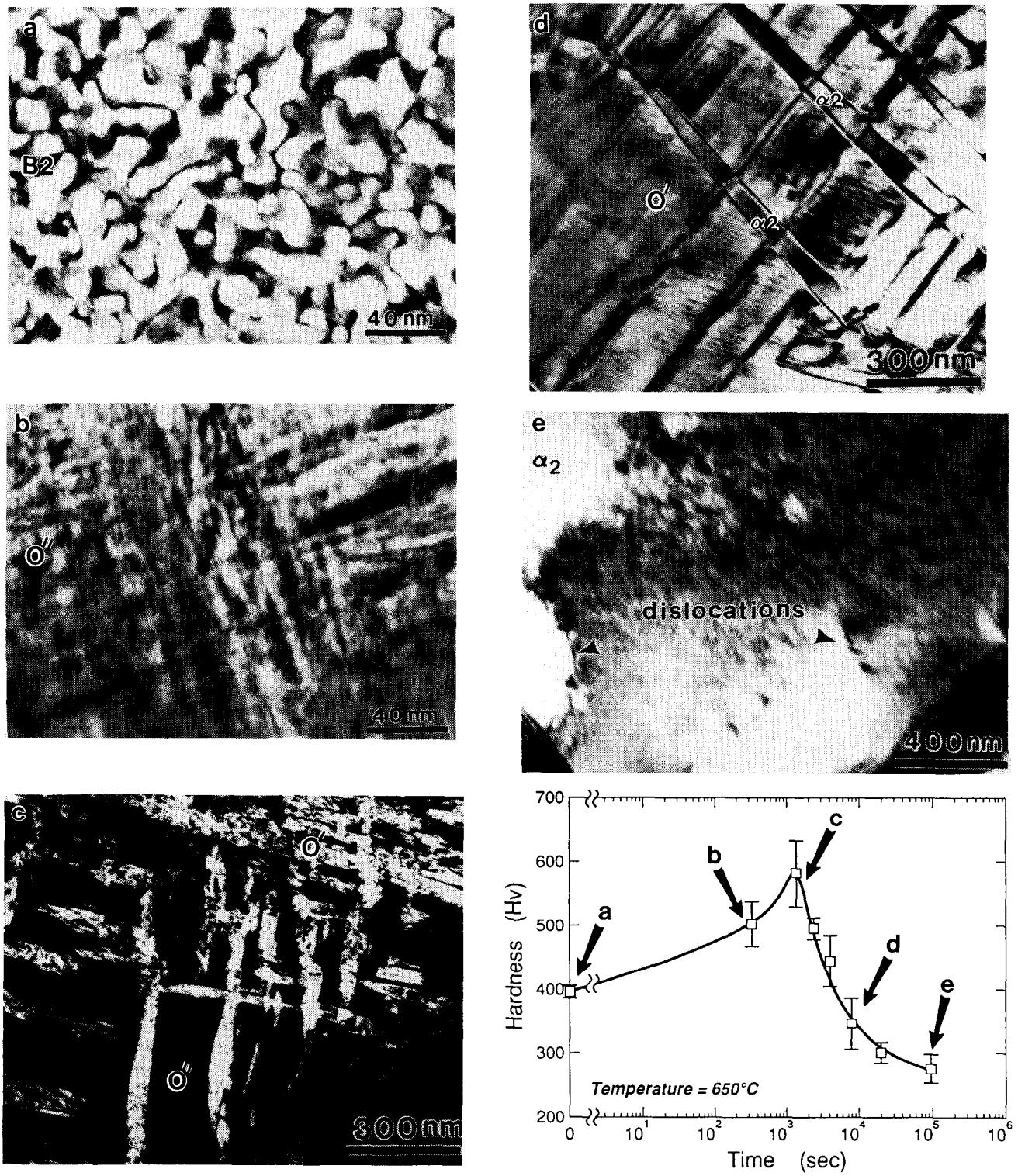


Fig. 7. Relationships between the hardness variation and microstructure evolution at 650 °C: (a)–(e) TEM images ((a) as-deposited, (b) 10 min, (c) 30 min, (d) 2 h, (e) 24 h); (f) hardness variation vs. aging time.

from powder samples aged at 650 °C is displayed in parallel with the microstructural evolution observed (by TEM) from foil samples aged at 650 °C. Fig. 7(a) is a dark-field image, generated from an as-deposited foil sample, showing a network of thermal antiphase boundaries (APBs) formed within the B2 phase. After aging at 650 °C for 10 min, the O″ phase with a martensitic-like morphology was observed as shown in Fig. 7(b). Fig. 7(c) is a dark-field image showing the formation of O′ laths within an O″ grain after aging at 650 °C for 30 min. Further aging caused the O′ lath to coalesce, and a plate-like $\alpha_2$ phase was found to grow within highly dislocated O′ grains after aging at 650 °C for 2 h (Fig. 7(d)). The microstructure contained mostly equiaxed $\alpha_2$ grains with few dislocations after aging at 650 °C for 24 h (Fig. 7(e)).

Clearly, the O′ phase appeared to be the hardest among all observed phases. This may be attributed to the existence of a high density of dislocations and stacking faults within the O′ phase. The hardness increased to a maximum (about 572 HV or 5.4 GPa) when the microstructure of the aged sample contained mostly O′ laths. This corresponds to an estimated yield strength of about 1.8 GPa. Subsequent aging resulted in a significant softening accompanied by the $O' \rightarrow \alpha_2$ transition. The hardness decreased (to about 260 HV or 2.6 GPa) when the microstructure contained mainly the equiaxed and nearly dislocation-free $\alpha_2$ grains. This corresponds to an estimated yield strength of about 870 MPa. These measurements and observations are somewhat in agreement with the findings reported in Ref. [10]: the estimated (room-temperature) yield strength of conventionally cast $\alpha_2$-base (Ti–24Al–11Nb) and RS O-base (Ti–23.5Al–25Nb) alloys were about 700 MPa and about 1 GPa, respectively. It is worth noting that the orthorhombic phases in the $(Ti,Nb)_3Al$ system have, depending on the chemical ordering and composition, four different derivatives: B19, O″, O′ and O ($Ti_2AlNb$); yet only the O ($Ti_2AlNb$) phase is considered to be fully ordered [3]. While the critical temperature (above which the O′ phase is unstable) may be dependent on the Nb content, the O ($Ti_2AlNb$) phase has been reported to remain stable up to about 1000 °C [11].

## 4. Conclusion

The time–temperature transformation behavior of rapidly solidified Ti–24Al–11Nb was studied between 450 and 800 °C using X-ray diffraction, electron diffraction, transmission electron microscopy, and microindentation methods. Age-hardening was found to accompany the $B2 \rightarrow O'$ transition. The hardness increased to a maximum (about 5.4 GPa) when the aged sample contained mostly O′ laths. Further aging resulted in a softening during the $O' \rightarrow \alpha_2$ transition. The hardness decreased to a minimum (about 2.6 GPa) when the microstructure had evolved to an equiaxed $\alpha_2$ structure. The results reveal that there exists a critical temperature (about 500 °C) above which the $B2 \rightarrow B19 \rightarrow O'' \rightarrow O' \rightarrow \alpha_2$ transitions take place, and below which the $O' \rightarrow \alpha_2$ reaction becomes very slow. That is, the O′ phase is kinetically stabilized at temperatures below about 500 °C.

## Acknowledgements

This work was co-sponsored by the Advanced Research Projects Agency (ARPA) (W. Barker, Program Manager) and the National Aeronautics and Space Administration (NASA) (R. Hayduk, Program Manager) through contract number NAGW-1692. The authors would like to thank Ms. W. Cai, a former research assistant, for her helpful work on microhardness measurements.

## References

[1] L.M. Hsiung, W. Cai and H.N.G. Wadley, *Acta Metall. Mater., 40* (1992) 3035.
[2] D. Banerjee, *Scripta Metall. Mater., 30* (1994) 855.
[3] B. Mozer, L.A. Bendersky, W.J. Boettinger and R.G. Rowe, *Scripta Metall. Mater., 24* (1990) 2363.
[4] L.M. Hsiung and H.N.G. Wadley, to be submitted to *Acta Metall. Mater.*, in preparation.
[5] L.A. Bendersky, A. Roytburd and W.J. Boettinger, *J. Res. NIST, 98* (1993) 561.
[6] L.M. Hsiung, W. Cai and H.N.G. Wadley, *Mater. Sci. Eng., A 152* (1992) 295.
[7] L.M. Hsiung and H.N.G. Wadley, *Scripta Metall. Mater., 26* (1992) 35.
[8] H.T. Weykamp, D.R. Baker, D.M. Paxton and M.J. Kaufman, *Scripta Metall. Mater., 24* (1990) 445.
[9] J.A. Peters and C. Bassi, *Scripta Metall. Mater., 24* (1990) 915.
[10] Editorial, *Adv. Mater. Proc., 141* (1992) 33.
[11] K. Muraleedharan, T.K. Namdi, D. Banerjee and S. Lele, *Metall. Trans. A, 23A* (1992) 417.